

Analytical and Neural Network Models for Gas Turbine Design and Off-Design Simulation[#]

Andrea LAZZARETTO* and Andrea TOFFOLO

Department of Mechanical Engineering - University of Padova

Via Venezia 1 - 35131 Padova – Italy

Tel: +039 049 827 6747, Fax: +039 049 827 6785

E-mail: andrea.lazzaretto@unipd.it

Abstract

This paper presents a gas turbine design and off-design model in which the difficulties due to lack of knowledge about stage-by-stage performance are overcome by constructing artificial machine maps through appropriate scaling techniques applied to generalized maps taken from the literature and validating them with test measurement data from real plants. In particular, off-design performance is obtained through compressor map modifications according to variable inlet guide vane closure. The set of equations of the developed analytical model is solved by a commercial package, which provides great flexibility in the choice of independent variables of the overall system. The results obtained from this simulator are used for neural network training: problems associated with the construction and use of neural networks are discussed and their capability as a tool for predicting machine performance is analyzed.

Key words: analytical model, neural network, design and off-design performance, gas turbine

1. Introduction

The increasing success of gas turbines in industrial applications (both electric and thermal energy production) is partly due to their quick response to load variations; in fact, these plants are often used for electric production in an intermediate range between peak and base demand.

Most gas turbine analytical models proposed in the literature are simply design models. Some others, however, are able to predict off-design behavior by means of zero-dimensional models (Ismail and Bhinder, 1991; Zhu and Saravanamuttoo, 1992), one-dimensional or more sophisticated models of the components (see e.g., Stamatis et al. 1990). The models are referred to as zero-dimensional if only the thermodynamic transformations across the component are considered without simulating the internal flow field. One-dimensional models include the variation of thermodynamic and flow quantities along the main flow direction.

The gas turbine design and off-design model presented in this paper aims both at computational simplicity and at the ability to deal with plants having large variations in the operating parameters. The main issue in the development of an off-design model is the prediction of machine off-design performance. The model should be constructed using the stage-stacking technique, simulating the performance maps of each machine stage, and then verified using operational data on single compressor and turbine stages. However, data about component performance maps are in general not available, since manufacturers very rarely supply gas turbine performance data to users. A mathematical model is therefore necessary to predict machine performance. In this paper generalized maps of the machines were taken from the literature and new maps for the considered gas turbines were constructed using appropriate scaling techniques. These maps are then to be validated on the basis of test measurement data of the whole machine. The numerical methods proposed by

[#] This paper was presented at the ECOS'01 Conference in Turkey, July 4-6, 2001 and revised.

* Author to whom all correspondence should be addressed.

Mirandola and Macor (1986) and Kurzke (1996) were used to manipulate compressor and turbine performance maps taken from the literature. The choice of using a single block to model the compressor through its performance maps implies that the VIGV effect is to be evaluated by modifying maps according to the VIGV degree of closure. Furthermore, the actual flow pattern of the turbine blade cooling system cannot be modeled properly (Zhu and Saravanamuttoo, 1992). Here, it was simplified with a single cooling air stream from compressor exit to the first turbine nozzle row. Load control was obtained by adjusting the VIGVs angle, while temperature at the turbine exit was kept constant. When the VIGVs reach maximum closure, further power reduction was obtained by decreasing fuel flow rate to the combustor (Lozza, 1996).

On the basis of these assumptions and of available actual plant test measurements data, a zero-dimensional design and off-design model of a single shaft gas turbine was developed. The set of equations was implemented for solving in a commercial package, Engineering Equations Solver (EES). This solver allows extreme flexibility in the choice of the decision variables for the whole system. While other softwares require explicit dependent variables and/or a defined order for equation system solution, there is no need in EES to replace component equations when the set of system independent variables is changed.

The results obtained from the model with different loads and different conditions of pressure and temperature at the compressor inlet were used to train neural networks (NNs), in order to test their ability to reproduce the relationships (generally non-linear) between the main operating parameters of the plant. During the training phase the NNs are taught to match a set of values of the variables given as inputs (load, pressure and temperature at the compressor inlet) with the corresponding values of the desired outputs (e.g. overall efficiency, compressor pressure ratio, air and fuel mass flow rates, as calculated by the analytical model). After the training, the NNs should provide satisfying predictions of the output variables, whether the values of the input variables belong to the training set or not. If a large measurement database had been available, these data could have been used to train the NNs directly, without the need to set up an analytical model that provides the large amount of data required to train a NN with several inputs.

2. Analytical Model

The thermal system to be simulated is a single shaft gas turbine for electricity production. The reference thermodynamic cycle is an open Brayton-Joule cycle, without regeneration.

A zero-dimensional analytical model was developed to predict the plant stationary behavior both in design and off-design conditions. The model considers the effect of variable inlet guide vanes (VIGVs) on compressor performance and a simplified turbine blades cooling system with a single cooling air stream from compressor exit to the first turbine nozzle row (*Figure 1*).

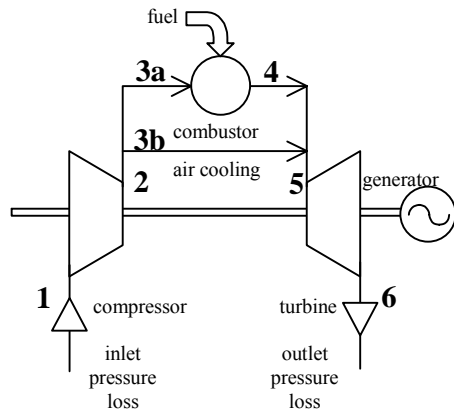


Figure 1. Plant Flowsheet

The chemical species involved (CH_4 , O_2 , N_2 , CO_2 , H_2O) were treated as ideal gases, with enthalpies and specific heats dependent from temperature only. The calculation of the thermodynamic properties of the mixture was performed according to the theoretical relations in Moran and Shapiro (1988) and Keating (1993), while enthalpy and entropy (at the reference pressure of 1.013 bar) values for each species were obtained from the JANAF tables. The fuel was assumed to be pure methane and the combustion model was taken from Keating (1993) and Turns (1996), considering a complete combustion of the fuel without dissociation. The air/fuel ratio and the fraction of combustion products were calculated from the adiabatic flame temperature.

The equations of the model express mass or energy balances of the components. The model calculates temperature, pressure and mass flow rate in each point of the plant (*Figure 1*).

Separate calculations are considered to construct the model in the design and off-design conditions, as shown in the following.

2.1 Design point model

The first step in the development of the model consists in determining the design point conditions. Ambient pressure and temperature (T_0 , p_0), compressor pressure ratio ($r_c = p_{02}/p_{01}$) and net power of the turbine (P_{tot}) were considered as independent variables. In addition to these variables one of the three following sets was chosen as inputs:

- $T_{05}, \eta_c, \eta_t;$
- $T_{06}, \eta_c, \eta_t;$
- $T_{06}, \eta_t, \dot{m}_1;$

where \dot{m}_1 is the air mass flow rate at the compressor inlet T_{05} , T_{06} are total temperature at turbine inlet and exit, respectively and η_c , η_t are compressor and turbine isentropic efficiencies, respectively. The choice was determined by the adjustment criterion that is used in partial load calculations (see Section 2.2.4).

Pressure losses were considered as assigned parameters concentrated in three points of the cycle:

- At the compressor inlet (filters and inlet duct);
- At the turbine outlet (silencer and discharge duct);
- In the combustion chamber.

The cooling air mass flow rate was assumed as constant (equal to 0.15) for all operation conditions. It was bled from the compressor outlet (point 2 in *Figure 1*) and sent to the first turbine nozzle row (point 5 in *Figure 1*). The compressor air bleed was only used to determine more precisely the combustion chamber parameters since the overall compressor and turbine performance maps already include the effects of the air cooling flows.

The temperature at the exit of the first nozzle (T_{05} in *Figure 1*) was considered as Turbine Inlet Temperature (TIT).

The equations of the model were written component by component. The independent variables at the component level which were not included in the set of independent variables of the total plant were considered as *calculated* variables. When for instance, the independent variables of the total plant are T_0 , p_0 , r_c , P_{tot} , T_{06} , η_c , η_t , the combustion adiabatic temperature T_{04} is a calculated variable for the combustion chamber. From the value of T_{04} , the excess air coefficient, the fuel mass flow rate and composition of the combustion products can be evaluated by the combustion chamber model. In the mixing point at the turbine inlet, T_{05} is considered as calculated variable and T_{04} is evaluated by the model. In the turbine model, the discharge temperature T_{06} is known and p_{06} is obtained from the discharge pressure losses; then, through the known efficiency η_t , the inlet conditions can be determined, including the value of T_{05} that was considered as calculated variable in the mixing point.

When the calculation of the thermodynamic quantities of the cycle is completed, the corrected compressor and turbine mass flow rates (ϕ_c and ϕ_t respectively) and the ratio Δh to T_{05} of the turbine

$$\phi_c = \frac{\dot{m}_1 \sqrt{T_{01}}}{p_{01}} ; \phi_t = \frac{\dot{m}_5 \sqrt{T_{05}}}{p_{05}} ;$$

$$\frac{\Delta h}{T_{05}} = \frac{h_{05} - h_{06}}{T_{05}} \quad (1)$$

are evaluated. These dimensional groups are needed in the off-design calculation to scale the available characteristic curves for the plant being considered.

2.2 Off-design model

2.2.1 Compressor maps. The calculation of the off-design conditions requires the off-design behavior of the compressor and turbine to be known. Starting from known maps, such as those shown in *Figure 2*, the evaluation of the off-design performance of different gas turbines can be investigated.

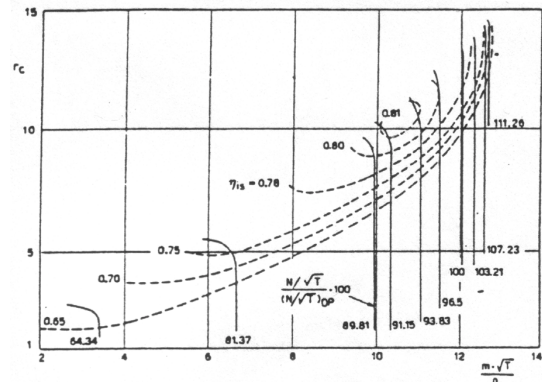


Figure 2. Compressor maps (Mirandola, Macor, 1986).

Maps of type as *Figure 2* cannot be directly used in a simulation program for two main reasons:

- in the asymptotic segment of the curves, assigned values for corrected speed and mass flow rate ($N/\sqrt{T_{01}}$ and $\dot{m}_1\sqrt{T_{01}}/p_{01}$, respectively) do not result in accurate values for the pressure ratio and efficiency;
- for low values of $N/\sqrt{T_{01}}$ and assigned value of the pressure ratio, two values of $\dot{m}_1\sqrt{T_{01}}/p_{01}$ may exist, as shown in *Figure 3* (Kurzke, 1996).

As suggested by Mirandola, Macor (1986) and Kurzke (1996), the problem is overcome by introducing auxiliary coordinates (lines β), having no physical meaning, which are superimposed to the characteristic curves as in *Figure 3*.

These lines are used to parameterize all the constant speed curves through a monotonic parameter β ranging from 0 to 1 (the auxiliary variable β becomes a dependent variable in the off-design model of the plant). Equally-spaced parabolic lines are chosen here, as suggested by Kurzke (1996). In this way, for given values of

$N/\sqrt{T_{01}}$ and β , the values of $\dot{m}_1\sqrt{T_{01}}/p_{01}$, r_c and η_c remain determined.

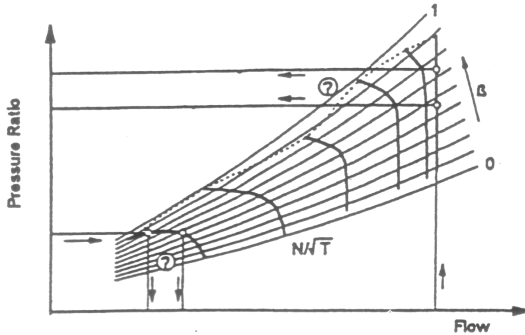


Figure 3. Auxiliary lines β used to read compressor maps (Kurzke, 1996).

Three maps in tabular form can then be obtained, in which the values of $\dot{m}_1\sqrt{T_{01}}/p_{01}$, r_c and η_c are included as functions of β and $N/\sqrt{T_{01}}$. These values are divided by the corresponding design point values to make the maps non-dimensional. TABLES I to III show the non-dimensional maps obtained by the compressor curves in Figure 2. When the maps are used for different compressors, their values are to be multiplied for the corresponding design point values (see also Walsh and Fletcher, 1998, Section 5.2.13).

Intermediate values of $\dot{m}_1\sqrt{T_{01}}/p_{01}$, r_c and η_c between two subsequent values of β and/or $N/\sqrt{T_{01}}$ are obtained by a two-dimensional linear interpolation.

TABLE I. COMPRESSOR NON-DIMENSIONAL CORRECTED AIR MASS FLOW.

(N/V T₀¹)%	64.34	81.37	89.81	91.15	93.83	96.50	100.00	103.21	107.23	111.26
β										
0.0	0.2808	0.5503	0.8271	0.8584	0.9182	0.9559	1	1.025	1.047	1.057
0.1	0.2808	0.5503	0.8270	0.8584	0.9182	0.9559	1	1.025	1.047	1.057
0.2	0.2808	0.5503	0.8270	0.8584	0.9182	0.9559	1	1.025	1.047	1.057
0.3	0.2808	0.5503	0.8270	0.8584	0.9182	0.9559	1	1.025	1.047	1.057
0.4	0.2808	0.5503	0.8270	0.8584	0.9182	0.9559	1	1.025	1.047	1.057
0.5	0.2808	0.5478	0.8270	0.8584	0.9182	0.9559	1	1.025	1.047	1.057
0.6	0.2799	0.5440	0.8264	0.8584	0.9164	0.9541	1	1.025	1.047	1.057
0.7	0.2752	0.5377	0.8239	0.8579	0.9151	0.9534	1	1.025	1.047	1.057
0.8	0.2672	0.5327	0.8208	0.8553	0.9120	0.9528	1	1.025	1.047	1.057
0.9	0.2547	0.5220	0.8132	0.8459	0.9057	0.9509	1	1.025	1.047	1.054
1.0	0.2358	0.5031	0.8050	0.8346	0.8962	0.9481	0.9994	1.024	1.044	1.052

TABLE II. COMPRESSOR NON-DIMENSIONAL PRESSURE RATIO.

(N/V T₀¹)%	64.34	81.37	89.81	91.15	93.83	96.50	100.00	103.21	107.23	111.26
β										
0.0	0.0098	0.2589	0.5012	0.5384	0.6279	0.6873	0.7546	0.8131	0.8654	0.8868
0.1	0.1306	0.2747	0.5321	0.5637	0.6524	0.7126	0.7759	0.8314	0.8812	0.8947
0.2	0.1386	0.2969	0.5622	0.5938	0.6809	0.7363	0.7997	0.8551	0.9042	0.9224
0.3	0.1449	0.3088	0.6017	0.6176	0.7047	0.7601	0.8234	0.8812	0.9303	0.9501
0.4	0.1584	0.3365	0.6170	0.6477	0.7324	0.7838	0.8511	0.9184	0.9501	0.9715
0.5	0.1639	0.3603	0.6572	0.6785	0.7601	0.8155	0.8749	0.9343	0.9818	0.9976
0.6	0.1821	0.3800	0.6809	0.7205	0.7918	0.8472	0.9105	0.9644	1.013	1.029
0.7	0.1900	0.3959	0.7047	0.7443	0.8155	0.8709	0.9343	0.9887	1.037	1.053
0.8	0.1979	0.4078	0.7284	0.7680	0.8393	0.8947	0.9660	1.017	1.065	1.082
0.9	0.2074	0.4196	0.7522	0.7918	0.8630	0.9264	1	1.053	1.101	1.116
1.0	0.2138	0.4276	0.7641	0.8068	0.8828	0.9541	1.037	1.082	1.124	1.140

TABLE III. COMPRESSOR NON-DIMENSIONAL ISENTROPIC EFFICIENCY.

(N/V T₀¹)%	64.34	81.37	89.81	91.15	93.83	96.50	100.00	103.21	107.23	111.26
β										
0.0	1.022	0.7962	0.8025	0.7898	0.8255	0.8255	0.7516	0.7006	0.6369	0.6115
0.1	0.8089	0.8025	0.8535	0.8408	0.8662	0.8599	0.8153	0.7898	0.7643	0.7261
0.2	0.8153	0.8318	0.9045	0.8981	0.9172	0.9045	0.8535	0.828	0.7898	0.758
0.3	0.828	0.8535	0.9427	0.9414	0.958	0.9554	0.8917	0.8662	0.828	0.7771
0.4	0.8316	0.8854	0.972	0.9809	0.9873	0.9745	0.9439	0.9146	0.8471	0.8153
0.5	0.8382	0.9172	0.9936	0.9975	1.009	0.9949	0.9682	0.9554	0.8828	0.8306
0.6	0.8433	0.9554	1.009	1.019	1.022	1.009	0.9873	0.9682	0.893	0.8662
0.7	0.8497	0.958	1.02	1.025	1.026	1.015	0.9936	0.9745	0.9236	0.879
0.8	0.8535	0.9605	1.027	1.032	1.032	1.019	0.9987	0.9732	0.9299	0.879
0.9	0.8535	0.9618	1.024	1.033	1.034	1.019	1	0.9809	0.9236	0.879
1.0	0.851	0.9618	1.022	1.031	1.032	1.018	0.9975	0.9873	0.9236	0.8917

2.2.2 Turbine maps. Turbine maps, such as those in Figure 4, need to be known for the off-design calculations.

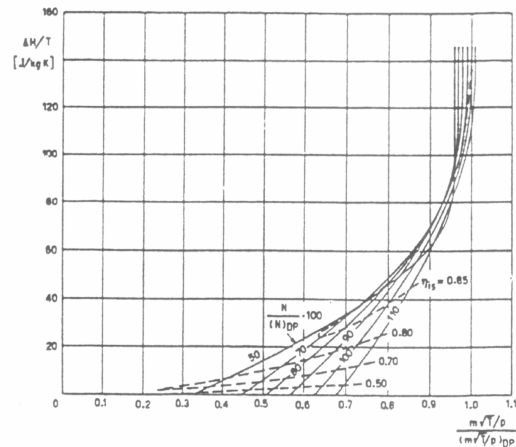


Figure 4. Turbine maps (Mirandola and Macor, 1986)

These maps express $\Delta h/T_{05}$ (see Eq. 1) and η_t as function of $\phi_t/(\phi_t)_{DP}$ and $N/\sqrt{T_{05}}$; auxiliary β lines are not needed for reading these maps which are transposed in tabular form to be used in the calculations.

As for the compressor, the values of ϕ_t and η_t between two subsequent values of $\Delta h/T_{05}$ and $N/\sqrt{T_{05}}$ are obtained using a two-dimensional linear interpolation.

2.2.3 Compressor maps under variations of the VIGVs angle. A variation in the inlet flow angle results in a modification of the fluid-dynamic behavior of the compressor and in the consequent modification of its characteristic curves. The indications by Walsh and Fletcher (1998, Section 5.2.8) can be used to modify the compressor maps for each value of the inlet flow angle (Figure 5). At low speed the speed lines move approximately horizontally and the surge line moves to the left. At high speed the effect of the VIGV angle makes the speed lines shift towards both lower pressure ratios and mass flow rates with only small improvement in surge limits. The efficiency map is modified according

to a criterion aimed at obtaining values close to the maximum ones in each load condition.

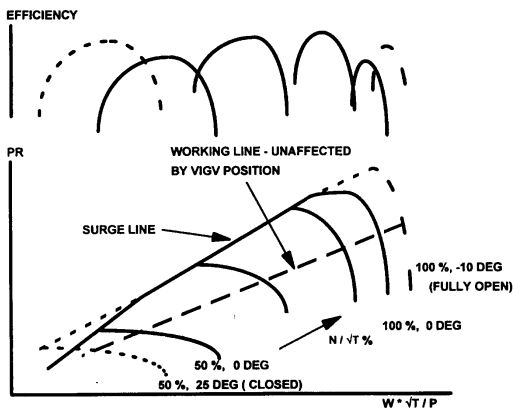


Figure 5.. VIGV effect on compressor maps (Walsh and Fletcher, 1998) (w indicates mass flow rate m_1)

2.2.4 Load adjustment criteria. Various load adjustment criteria can be adopted in the plant operation (see Cohen, 1972, Desideri, Facchini, 1989, Bathie, 1984, Lozza 1996, Walsh, Fletcher, 1998). The simplest criterion consists in lowering the fuel mass flow rate in the combustion chamber, the air mass flow rate remaining constant (no VIGV adjustment in this case). This criterion results, however, in a decrease of the turbine inlet temperature with a strong reduction in overall efficiency. More common is the load adjustment with VIGVs that is considered here: in the first part of load reduction, the turbine outlet temperature is kept constant while the power reduction is obtained by closing the VIGV angle (and consequently lowering the air mass flow rate); when the minimum VIGV angle is reached, the fuel mass flow rate is decreased by the control system until the desired power output is obtained.

2.2.5 Off-design calculations. All the thermodynamic quantities calculated at the design point (Section 2.1) are known before performing the off-design calculations. In the first part of load reduction a value is assigned to the variable α_{IGV} which mathematically describes the VIGV effect, and the turbine outlet temperature T_{06} , which is a controlled variable, is kept constant at the design point value. Ambient temperature and pressure are independent variables fixed as parameters; the value of $N/\sqrt{T_{01}}$ is therefore known.

By giving r_c a guess value (it is a calculated variable - see Section 2.1- and its value will be calculated by the turbine model), the values of β , η_c and $\phi_c = \dot{m}_1 \sqrt{T_{01}} / p_{01}$ can be obtained by the compressor maps. From ϕ_c and the pressure losses

at the compressor inlet, p_{01} and \dot{m}_1 are evaluated, so that the thermodynamic conditions at point 2 and the air cooling flow rate ($0.15\dot{m}_1$) can also be determined. The calculations of the other points in the cycle are then performed as already shown for the design point calculations under the hypothesis of constant T_{06} (see Section 2.1), by considering T_{04} and T_{05} as calculated variables for the combustion chamber and the mixing point, respectively. These temperatures are then evaluated in the mixing point and turbine models, respectively. In the turbine model an iterative procedure to evaluate T_{05} is needed as described below. From the inlet and outlet thermodynamic conditions (p_{05} is evaluated in the combustion chamber model, T_{06} is fixed by the adjustment system and p_{06} is evaluated from the discharge pressure losses), the efficiency η_t is determined. The value of $\Delta h/T_{05}$ is then read from the turbine map and is used to update the guess of T_{05} until convergence is obtained. Then, the value of $\phi_t = \dot{m}_5 \sqrt{T_{05}} / p_{05}$ is obtained from the mass flow rate map. By expressing p_{05} as a function of the pressure ratio r_c , $p_{05} = p_{01} r_c - \Delta p_{CC}(r_c)$, and substituting into ϕ_t , the value of r_c is calculated.

3. Example of Application

The model presented in the previous sections was implemented in a commercial equation solver (Engineering Equations Solver – EES). The flexibility in writing and solving equations provided by EES, made it possible to include various options in the choice of the independent variables, and then to simulate different plant adjustment modes (see Section 2.2.4).

TABLE IV. WORKING PARAMETERS AT DESIGN POINT.

Power output at coupling	$P_{tot}=61.54 \text{ MW}$
Rotational speed	$N=3000 \text{ rpm}$
Pressure ratio	$r_c=15.6$
Turbine inlet temperature	$T_{05}=1120 \text{ }^\circ\text{C}$
Turbine outlet temperature	$T_{06}=533.6 \text{ }^\circ\text{C}$
Air mass flow rate at compressor inlet	$\dot{m}_1=183.3 \text{ kg/s}$
Cooling air mass flow rate	$\dot{m}_{3b}=27.5 \text{ kg/s}$
Compressor outlet temp.	$T_{02}=397.5 \text{ }^\circ\text{C}$
Fuel mass flow rate	$\dot{m}_f=3.438 \text{ kg/s}$
Mechanical efficiency (turbine to compressor)	$\eta_m=0.985$
Fuel low heating value	$LHV=50056 \text{ kJ/kg}$
Ambient pressure and temperature (ISO-standard reference conditions)	$p_0=1.013 \text{ bar}$ $T_0=15^\circ\text{C}$

The EES method to solve the system of non-linear equations is a variant of Newton's method (EES, 1999). The Jacobian matrix needed in Newton's method is evaluated numerically at each iteration. Sparse matrix techniques are employed to improve calculation efficiency and permit rather large problems to be solved. The efficiency and convergence properties of the solution method are further improved by the step-size alteration and implementation of the Tarjan blocking algorithm which breaks the problems into a number of smaller problems which are easier to solve. A higher number of blocks is desired to obtain the convergence more easily. This number mainly depends on the choice of the independent variable set and, in turn, on the adjustment mode.

To check the simulation capabilities of the analytical model, the results were compared with design and off-design working parameters of a single shaft 60 MW commercial gas turbine. The design point values are shown in TABLE IV

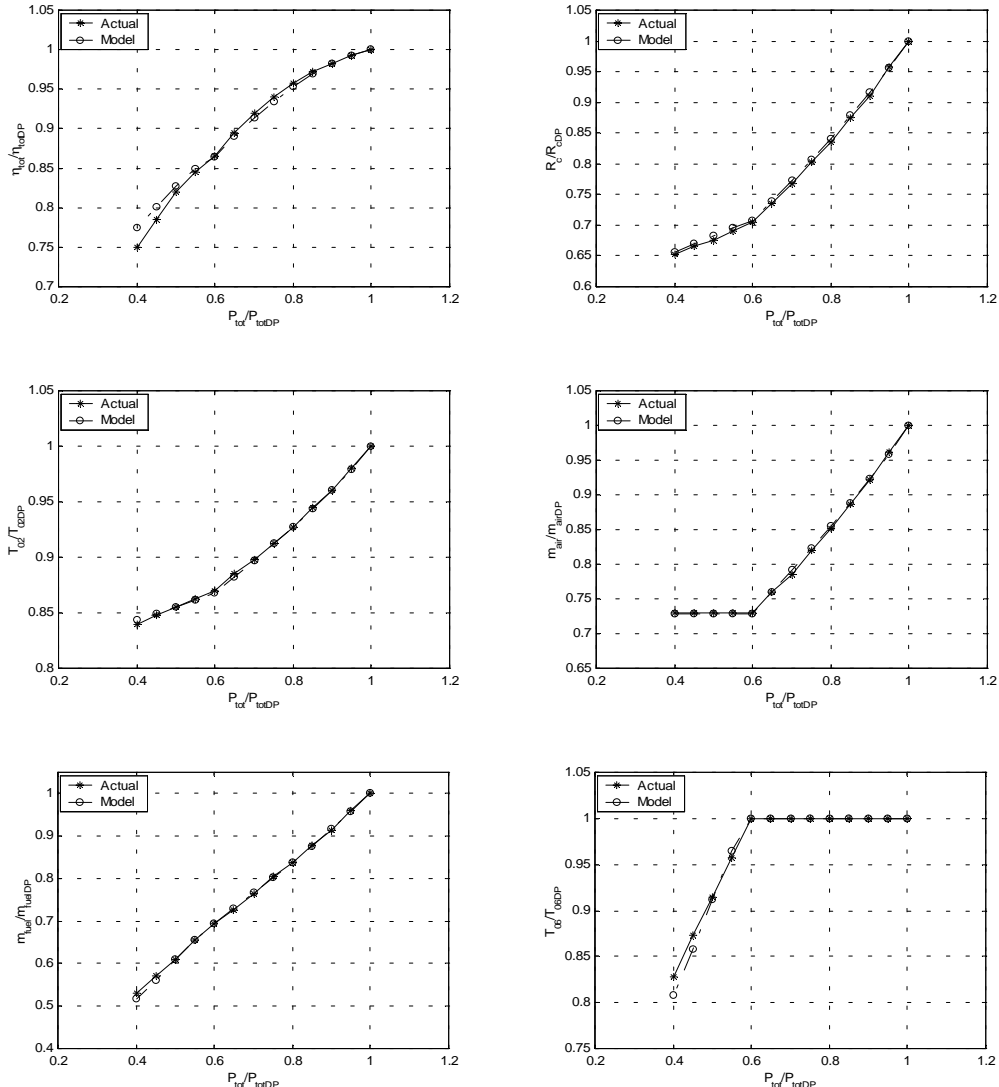


Figure 6. Comparison between simulated and actual off-design values along the working line.

(according to these values the compressor isentropic efficiency is 0.8543).

The variables r_c , P_{tot} , T_{06} , \dot{m}_1 , p_0 , T_0 , and LHV were assumed as independent. The values of the other variables are obtained by the model using $\eta_i=0.88$ and 2% p_0 , 3% p_{06} and 3% p_{03} as pressure losses at compressor inlet, turbine outlet, and in the combustion chamber, respectively.

In the off-design calculations the existing maps of a GE LM 2500 compressor and turbine (Figures 2 and 4) were used to build generalized non-dimensional maps in tabular form which were updated by scaling to get the desired design point values. All pressure losses (at compressor inlet, turbine outlet, and in the combustion chamber) were assumed to be a quadratic function of mass flow rate.

The effect of the VIGV angle was considered by moving horizontally the compressor speed lines while reducing their vertical extension to keep the upper point on the surge line (this line is supposed to remain unchanged in the off-design operation). The horizontal shift is proportional to the value of α_{IGV} and can be determined when the maximum VIGV closure and the corresponding air mass flow rate are known. At increasing VIGV closure degrees, the efficiency curves were modified to get, at each VIGV angle, an expected working point efficiency close to its maximum value, according to the indications given by Walsh and Fletcher (1998) (see *Figure 5*).

A partial load simulation was then performed, the results of which represent the plant working line. In general, some deviations can be found by this first simulation on the values of one or more thermodynamic parameters along the working line. To make the working line parameters match more accurately with the actual ones, the following actions were then undertaken: i) the pressure ratio and mass flow rate as function of load were tuned by modifying the turbine map; ii) the compressor outlet temperature T_{02} was adjusted by modifying the compressor efficiency map and/or its shift caused by the VIGV closure. Since a change in T_{02} unavoidably reflects on the turbine map through T_{05} , an iterative adjustment was needed.

A comparison between off-design simulated and actual values is shown in *Figure 6*. A satisfactory approximation was obtained for all the represented variables. The little error still existing when the maximum VIGV closure is reached could be corrected with further maps adjustments.

4. The Neural Network Model

Artificial NNs are a well-known tool among artificial intelligence techniques able to reproduce the relationships existing between input and output variables of (highly) non-linear system. Thus, they can be used to predict the performance of a gas turbine plant, setting up a model that is alternative to the analytical one.

Once the structure has been chosen, the training phase performed and the outputs validated, a NN offers the advantage of a much lower computational effort. In fact, the number of operations required is minimal with respect to the analytical model, whose non-linear set of thermodynamic equations usually requires an iterative algorithm to be solved. Another advantage of a NN is its intrinsic ability of adaptation to a given plant. While the analytical model has to be “tuned” to have its output represent accurately the behavior of the plant, a NN already adjusts its output implicitly during the training phase. However, the NN approach to the simulation of a real plant can only be considered for a stand-alone

model if a large number of data related to the desired input and output variables is available.

The setup of a NN requires the choice of the number of layers, the number of neurons in each layer, the transfer function of each layer and the training algorithm (Fausett, 1994). Two phases are then required to make the NN become operative. The first one is the training (or learning) phase, in which the NN is taught to match a known set of corresponding input and output values. This allows the NN to “learn” the relationship existing between inputs and outputs. During the learning process, “learning” is achieved through modification of weights associated with each neural connection made by the training algorithm (also called “learning rule”). The training process aims, in general, at the minimization of the error between predicted and actual values. This phase is the most time consuming and it is critical for the success of the NN as a predictive model. The second phase is called generalization (or testing). Here, the NN is tested on another known set of corresponding input and output values different from the training set and the performance is evaluated (Fausett, 1994; Baughman and Liu, 1995).

4.1 Application to the gas turbine

The NN approach (see, e.g., Chbat et al., 1996, Kanelopoulos et al., 1997) was used to predict the operation of the gas turbine plant considered in the previous sections at different loads and environmental conditions, which univocally define the working point of the plant. Ambient pressure (p_0) and temperature (T_0), and plant output power (P_{tot}) were therefore chosen as input variables to the NN (*Figure 7*).

The output variables were chosen among the thermodynamic quantities that are usually measured in a real plant: compressor outlet temperature (T_{02}), turbine outlet temperature (T_{06}), compressor inlet mass flow rate (\dot{m}_1), fuel mass flow rate to the combustor (\dot{m}_f), compressor pressure ratio (r_c). In a real plant, the latter is calculated by the data acquisition system as the ratio between compressor outlet and inlet pressures. Other useful quantities, characteristic of the thermodynamic cycle, were then added to the set of output variables: the overall efficiency (η_{tot}), excess air coefficient (L) and turbine inlet temperature (T_{05}).

The data required for the training phase were supplied by the analytical off-design model developed in Section 2. Otherwise, if a large database of measurements had been available for the desired variables, the training would have been performed directly.

Simulations were performed with p_0 ranging from 98kPa to 104kPa by steps of 1kPa, and with T_0 ranging from 0°C to 40°C by steps of 5°C; twenty different load conditions were simulated for each pair of p_0 and T_0 , making a total of 1260 samples available for the training.

A simple two-layer feed-forward topology was chosen as a compromise between short learning time and good prediction accuracy (*Figure 7*).

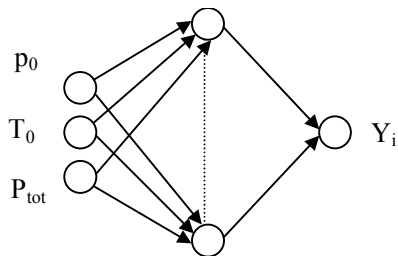


Figure 7. Neural network topology for a generic plant variable Y_i .

A NN was set up for each output variable (T_{02} , T_{05} , T_{06} , \dot{m}_1 , \dot{m}_f , r_c , L , η_{tot}) using the MATLAB Neural Network Toolbox (MATLAB, 2000). The output layer is therefore made up of only one neuron, while the number of neurons in the hidden layer is a trade-off between the learning time and the generalization ability of the NN. An output layer including all the output variables (Kanelopoulos et al., 1997) increases the computational effort, while decreasing, in general, prediction accuracy if a large number of data is not available for training. The transfer function used in the hidden layer was always the hyperbolic tangent sigmoid function. Conversely, the linear transfer function was sometimes used in the output layer instead of it (see TABLE VI). The learning rules used were the BFGS quasi-Newton and the Levenberg-Marquardt backpropagation algorithms (MATLAB, 2000).

To increase the efficiency of the learning procedure, the training data set values are normalized in the range [-1,1] (Baugham and Liu, 1995). The number of samples used to form the training set is kept as low as possible, considering the need of covering the entire ranges of the input variables. In TABLE V the pairs of p_0 and T_0 used in the off-design simulations are shown: gray squares represent the samples chosen to build up the training set, while black squares represent the samples of the test set; for each pair of p_0 and T_0 all the twenty simulations at different load conditions were used, so a total of 620 samples were used in the training phase and 240 in the generalization phase.

TABLE V. TRAINING AND TEST SET.

		T_0 [°C]								
		0	5	10	15	20	25	30	35	40
p_0 [kPa]	98									
	99									
	100									
	101									
	102									
	103									
	104									

TABLE VI presents the configurations giving the highest accuracy for each NN in terms of number of neurons in the hidden layer, transfer functions and training method used, and maximum percentage error found in the generalization phase (referred to the non-normalized output quantities), that is $\text{err}\% = (\bar{x}_{\text{NN}} - \bar{x}_{\text{actual}})/\bar{x}_{\text{actual}}$.

TABLE VI. HIGHEST ACCURACY NEURAL NETWORKS.

Network	No. of neurons in the hidden layer	Hidden layer Transfer function	Output layer Transfer function	Learning algorithm	Maximum Percentage Error
η_{tot}	15	hyperbolic tangent sigmoid	hyperbolic tangent sigmoid	BFGS	1.05
R_c	15	hyperbolic tangent sigmoid	hyperbolic tangent sigmoid	Levenberg-Marquardt	0.79
\dot{m}_1	15	hyperbolic tangent sigmoid	hyperbolic tangent sigmoid	Levenberg-Marquardt	0.47
T_{02}	21	hyperbolic tangent sigmoid	linear	Levenberg-Marquardt	0.3
T_{03}	18	hyperbolic tangent sigmoid	linear	Levenberg-Marquardt	0.13
T_{05}	14	hyperbolic tangent sigmoid	hyperbolic tangent sigmoid	Levenberg-Marquardt	0.49
\dot{m}_f	9	hyperbolic tangent sigmoid	linear	Levenberg-Marquardt	0.92
L	12	hyperbolic tangent sigmoid	hyperbolic tangent sigmoid	BFGS	0.99

Figures 8 and 9 show a comparison between off-design total plant efficiencies obtained by the neural network and the analytical model for different normalized values of P_{tot} and T_0 . The highest prediction errors are around 1% for all the considered variables as it appears from the corresponding percentage errors (TABLE VI).

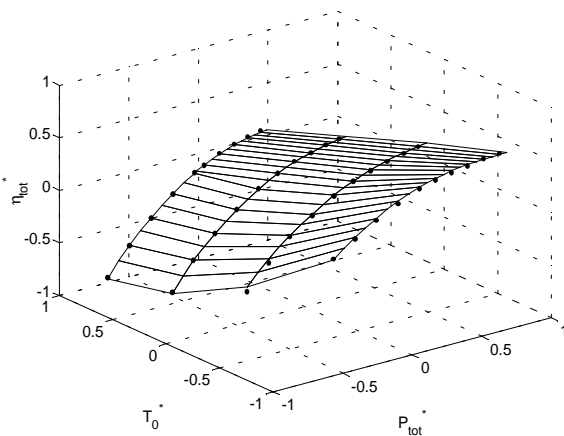


Figure 8. Comparison between NN prediction (surface) and model values (dots) for η_{tot}

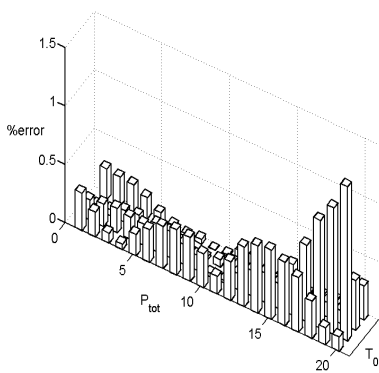


Figure 9. Percentage deviation of NN predictions for η_{tot} from actual values.

5. Conclusions

Two approaches to a zero-dimensional design and off-design model of a single-shaft gas turbine were presented and discussed.

The model obtains off-design performance from compressor and turbine generalized non-dimensional maps. Little errors on all the thermodynamic variables along the working line were achieved by the following actions: i) design point calculations and scaling of generic available compressor and turbine maps to get the design point, ii) compressor map modifications to take into account VIGV effects, iii) partial load simulation to determine an approximate engine working line, iv) tuning of both compressor and turbine maps to minimize differences between actual and simulated values of the parameters along the working line.

The analytical model was implemented using a commercial equation solver. High flexibility in the choice of the adjustment criteria is allowed by the different sets of independent variables that can be selected according to the available data.

Precise results were obtained notwithstanding only overall component characteristics were

considered. This approach, however, does not allow to take into account effects of internal parameters variations on performance.

Feed-forward neural networks, using limited computational effort, have shown to reproduce effectively actual working parameters with prediction accuracy of about one per cent. The most interesting feature of this approach is the ability of prediction of the output variables without any knowledge of the equations governing the main phenomena within the system. The use of NNs is an example of the application of artificial intelligence techniques to thermal system simulation. Their reliability in reproducing the relationships existing among the most important thermodynamic parameters may be a key point in their use in the simulation of complex thermal systems.

References

- Bathie, W. W., 1984, *Fundamentals of Gas Turbines*, John Wiley and Sons, Inc.
- Baughman D. R., Liu Y. A., 1995, *Neural Networks in Bioprocessing and Chemical Engineering*, Academic Press.
- Chbat N. W., Rajamani R., Ashley T., 1996, "Estimating Gas Turbine Internal Cycle Parameters Using a Neural Network", ASME 96-GT-316.
- Cohen, H., Rogers, G.F.C., Saravanamuttoo H.I.H., 1972, *Gas Turbine Theory*, Longman, London.
- Desideri U., Facchini B., 1989, (in Italian), "Analisi dei Sistemi di Regolazione nei Cicli Combinati Gas Vapore per la Produzione di Energia Elettrica" Third National Conference on Combined Power Plants, Pitagora Ed., Bologna - Italy.
- EES, 1999, "Engineering Equation Solver User's Guide", F. Chart Software, Middleton, Wisconsin, - USA.
- Fausett L., 1994, *Fundamentals of Neural Networks: Architectures, Algorithms and Applications*, Prentice-Hall.
- Ismail I.H., Bhinder F.S., 1991, "Simulation of Aircraft Gas Turbine Engines", ASME Journal of Engineering for Gas Turbines and Power, Vol.113, pp.95-99.
- Kanelopoulos, K., Stamatidis, A., Mathioudakis, K., 1997, "Incorporating Neural Networks into Gas Turbine Performance Diagnostics", ASME 97-GT-35.
- Keating, E., L., 1993, *Applied Combustion*, M. Dekker, Inc., New York.
- Kurzke, J., 1996, "How to get component maps for aircraft gas turbine performance calculations". ASME 96-GT-164.
- Lozza G., 1996, (In Italian), *Turbine a Gas e Cicli*

- Combinati*, Progetto Leonardo, Bologna - Italy.
- MATLAB User's Guide – Neural Network Toolbox, 2000, The Mathworks, Natick, MA.
- Mirandola, A., Macor, A., 1986, "Full Load and Part Load Operation of Gas Turbine-Steam Turbine Combined Plant", ISEC, Vol.VIII-15.
- Moran M., Shapiro, H., 1998, *Fundamentals of Engineering Thermodynamics*, John Wiley and Sons Ltd, New York, NY.
- Stamatis, A., Mathioudakis, A., 1990, Adaptive Simulation of Gas Turbine Performance, Journal of Engineering for Gas Turbine and Power, Vol.112, pp. 168-174.
- Turns S.R., 1996, *An Introduction to Combustion*, Mc Graw-Hill.
- Walsh P.P., Fletcher P., 1998, *Gas Turbine Performance*, Blackwell Science Ltd, Oxford, UK.
- Zhu P., Saravanamuttoo, H.I.H., 1992, "Simulation of an Advanced Twin Spool Industrial Gas Turbine", Journal of Engineering for Gas Turbine and Power, Vol.114, pp. 180-186.